Progress In Electromagnetics Research C, Vol. 85, 9–23, 2018

Miniaturized Beam-Switching Array Antenna with MIMO Direct Conversion Transceiver (MIMO-DCT) System for LTE and Wireless Communication Applications

Yasser M. Madany[1], Roshdy A. Abdelrassoul[2, *], and Nahla Mohamed[3]

Abstract—Due to the increase in the data rates for modern wireless communications and recent generation standards, the switched beam approach and multiple-input multiple-output (MIMO) direct conversion transceiver (MIMO-DCT) have become promising techniques to satisfy these requirements. The combining of switched beam and MIMO-DCT through the use of multiple antenna elements has been investigated to overcome the high complexity and high spatial directivity of the conventional system. In this paper, a low cost miniaturized beam-switching array antenna with a MIMO-DCT system has been proposed, designed and analysed. The entire proposed system structure has two design stages. The first is the design of MIMO-DCT via the integration of microstrip antenna element, hybrid coupler, Wilkinson power divider and single-pole double-throw (SPDT) transmitter/receiver (T/R) switch. The second has the switched beam array antenna design using a Butler matrix feeding network and four distributed subarrays (DSs) of the MIMO-DCT. The entire proposed design structure components have been optimized using a commercial software to evaluate each component and meet the desired performance. The final proposed two-stage design has been fabricated, integrated, and the radiation characteristics have been demonstrated, using the Agilent FieldFox network analyser, to meet the requirements for LTE and wireless communication applications.

1. INTRODUCTION

In the DCT, the system supports multiple modes of operation, the ability to eliminate the IF stage and the need for multiple filters comparable with the conventional system. Also, the DCT has many advantages over the conventional system, such as low power consumption, high fidelity, functionality and reducing latency with relatively large dynamic range [1, 2]. The SPDT-T/R switch is a block module that only has a single input antenna and can connect to and switch between two outputs for transmitter or receiver path [3]. The concept topology of the MIMO-DCT design has been a major research area in the past few years [4, 5]. To change the beam in several angles, the most suitable approach is using a switched beam system [6–9]. The switched beam approach plays an important role in transmitting and receiving modes by subdividing the entire array antenna into micro-sectors to improve the capacity during the transmitting mode and point the main beam to the optimal direction at the receiving mode. In this paper, the investigation and design of a miniaturized beam-switching array antenna with a MIMO-DCT system and switched Butler matrix network is introduced. The proposed system design structure has been designed using a Rogers RO3210 substrate with $\varepsilon_r = 10.2$, $\tan\delta = 0.003$ and thickness of 1.27 mm. The radiation characteristics of the proposed system are illustrated and analysed using HFSS simulator. The proposed fully integrated MIMO-DCT with Butler matrix system has been

Received 10 May 2018, Accepted 15 June 2018, Scheduled 24 June 2018

* Corresponding author: Roshdy A. Abdelrassoul (roshdy@ieee.org).

[1] Electrical Engineering Department, Alexandria University, Alexandria, Egypt. [2] Electronics and Communications Engineering Department, Arab Academy for Science and Technology (AAST), Alexandria, Egypt. [3] Electronics and Communications Engineering Department, Arab Academy for Science and Technology (AAST), Alexandria, Egypt.

fabricated and measured using the FieldFox network analyser, and the observation frequency sweep band is UWB from 1–10 GHz.

2. PROPOSED MIMO-DCT COMPONENTS STRUCTURE

The MIMO-DCT design structure is introduced in this section, and the main operating frequency is around 3 GHz. The proposed MIMO-DCT has four main components entitled microstrip antenna element, SPDT-T/R switch, 90° hybrid coupler and Wilkinson power divider.

2.1. Antenna Element

The rectangular microstrip antenna (RMA) has been designed and analysed. The proposed antenna element has an inset feed to improve the impedance matching at the desired frequency. The 3D and top views of the proposed antenna as well as its dimensions are shown in Fig. 1(a). The radiation characteristics for the proposed antenna, such as S_{11}, 2D far-field radiation patterns and the 3D polar plot patterns of the total far field, E_{tot} and total gain, G_{tot}, are shown in Fig. 1(b).

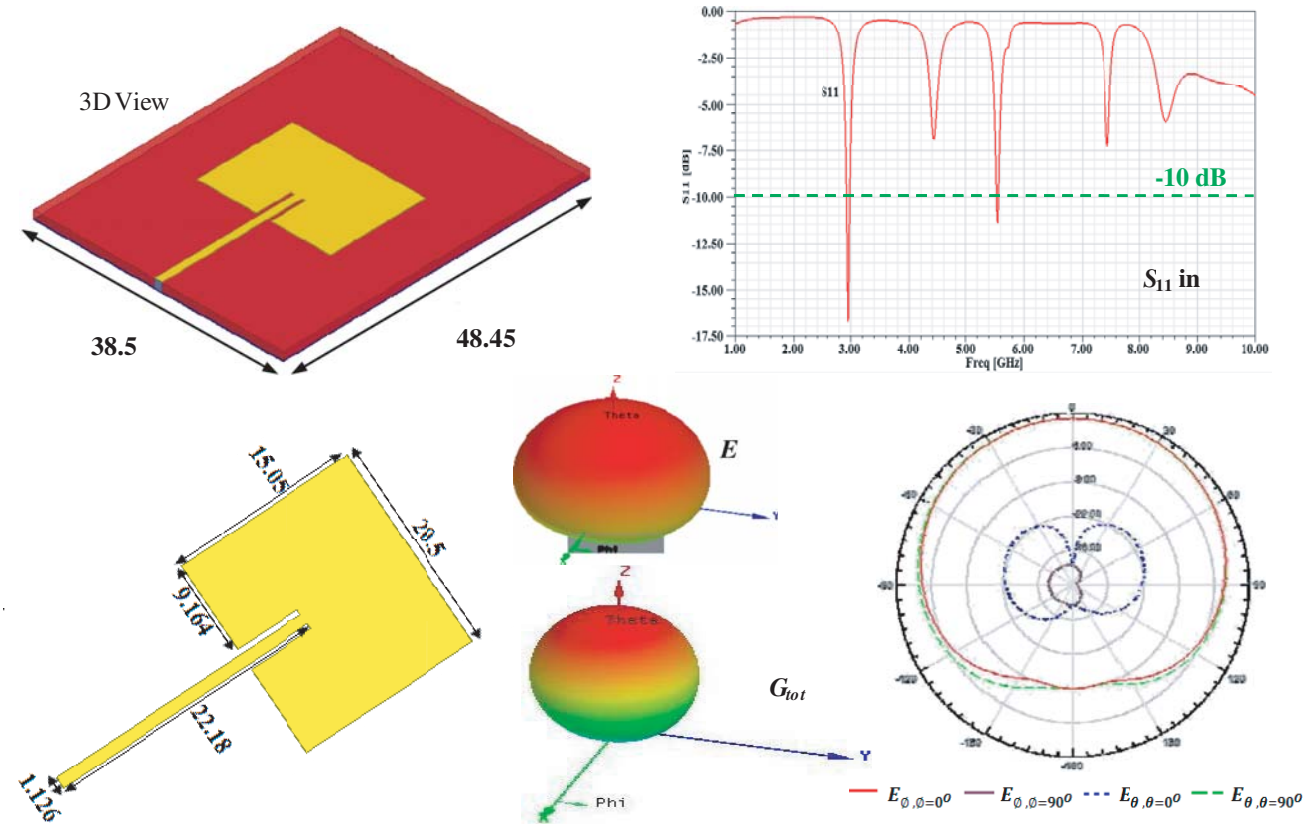

(a) (b)

Figure 1. Proposed RMA and simulation results (all dimensions in mm). (a) RMA views. (b) Radiation characteristics.

2.2. SPDT-T/R Switch

A typical behaviour of the SPDT-T/R switch has two operation modes. For the transmitting side, the transmitted RF signal passes through the active output port, *active mode*, from transmitter to antenna. While at the same time, the other output port is a nonactive port, *isolation mode*, to prevent leakage RF of that signal to pass into the front-end of receiver [3] and vice versa at the receiving side.

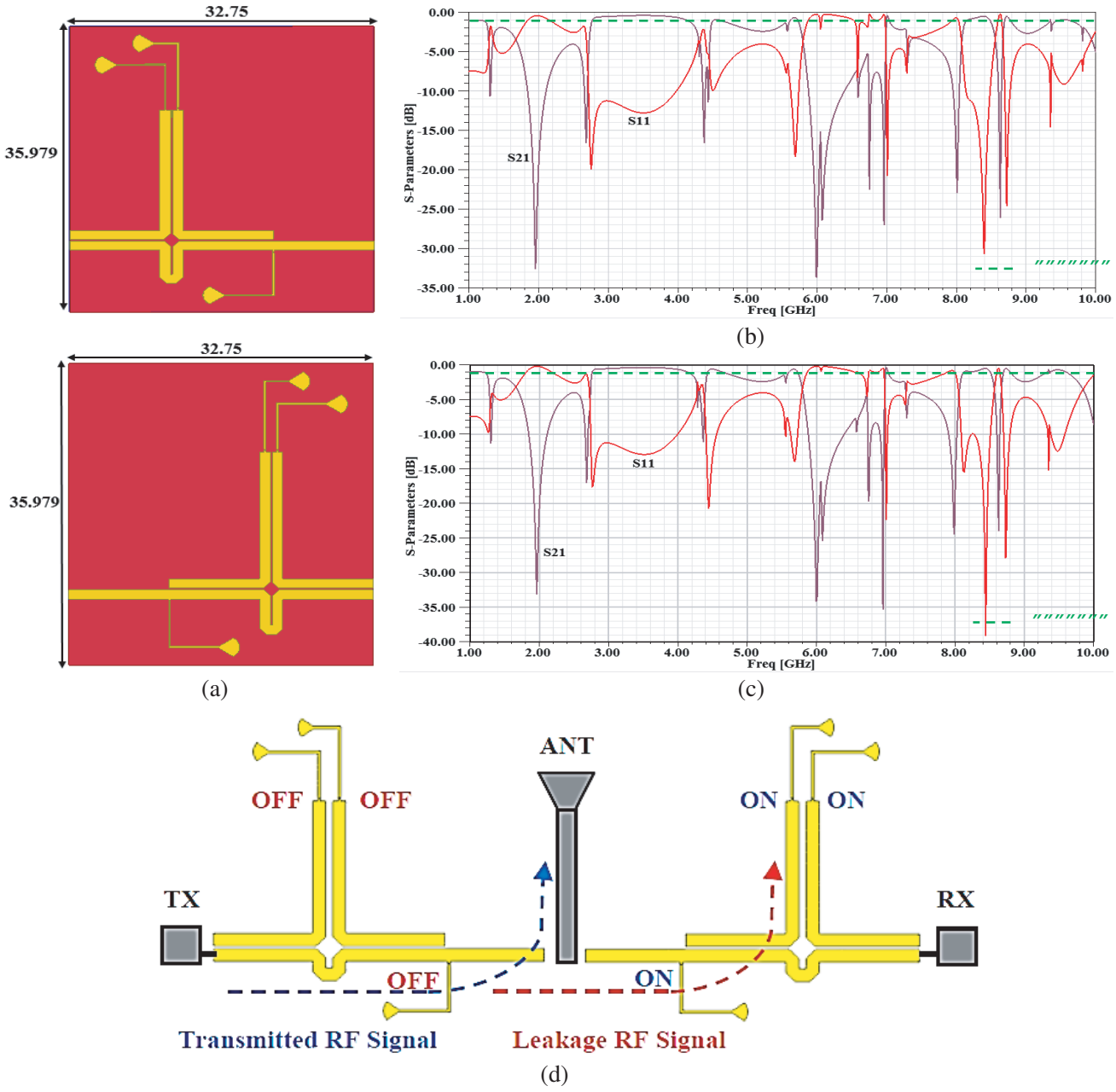

Figure 2. Proposed SPDT-T/R switch and simulation results. (a) The proposed SPDT switch. (b) Transmitting (Tx) side. (c) Receiving (Rx) side. (d) The proposed SPDT switch in transceiver system.

Figure 2(a) shows the proposed SPDT switch. Figs. 2(b) and (c) show the simulated S-parameters characteristics of the identical SPDT-T/R switch structures, for the transmitting and receiving sides, and Fig. 2(d) shows the complete proposed SPDT switch in transceiver system. Referring to [3], the proposed SPDT-T/R switch has been designed, and the dimension details have been illustrated in Fig. 3(a). The basic behaviours of the proposed SPDT-T/R for the two operation sides show wideband RF properties in terms of low transmission losses (S_{21} or $S_{12} \leq -1$ dB, ON state) and high isolation (S_{21} orS_{12}, OFF state) over a relatively wide frequency range. From Fig. 2(d), the SPDT behaviour was found that, in the transmitting mode, RF signals go through transmitter to the proposed antenna, and the PIN diodes are turned 'OFF'. Then, the SPDT coupled-resonator becomes all-pass response while in the receive arm, the PIN diodes are turned 'ON'. Then, the SPDT coupled-resonator becomes

band-stop response. Hence, the additional isolation can be obtained, and also the receive arm becomes an absorptive port. The same operation can be obtained in the receiving mode where the RF signals go through the proposed antenna to receiver when PIN diodes are turned 'ON' in the transmit arm, and PIN diodes are turned 'OFF' in the receive arm. The proposed integrated antenna with an identical SPDT-T/R module is shown in Fig. 3.

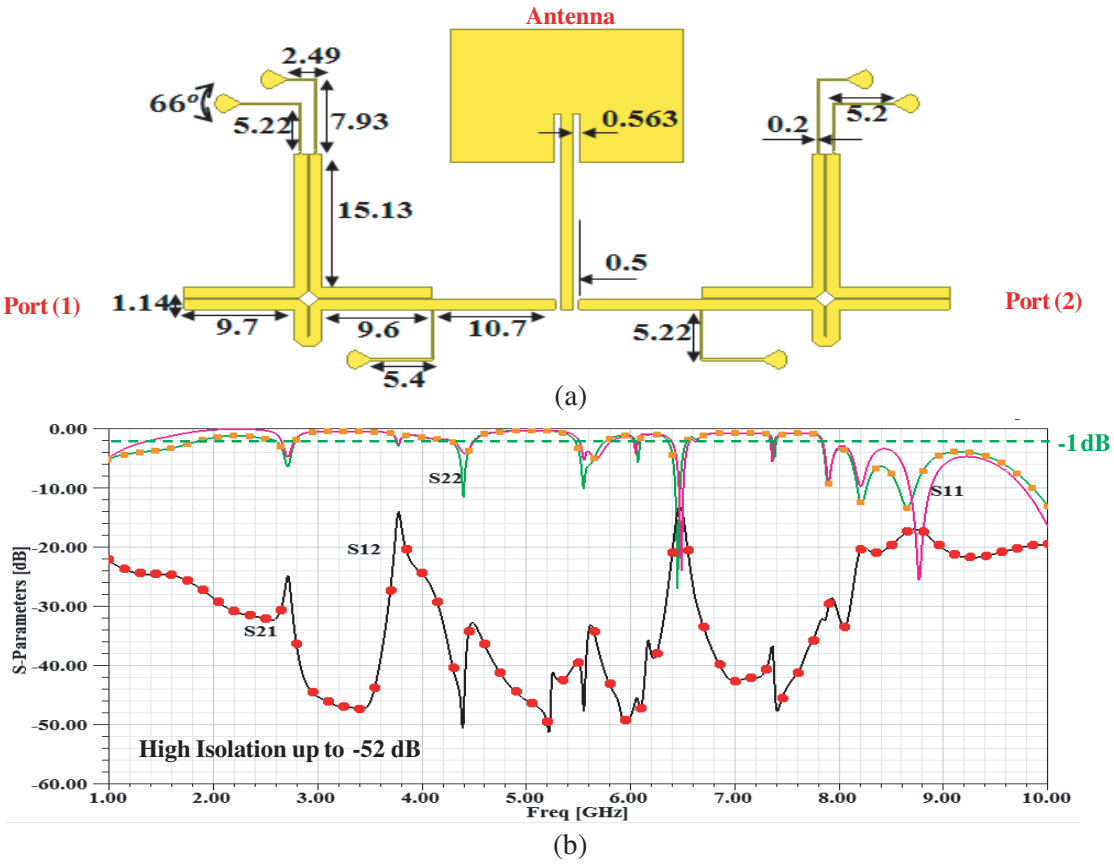

Figure 3. Proposed antenna with SPDT-T/R module and simulation results (all dimensions in mm). (a) Top view design structure. (b) S-parameters in dB.

Figure 3 shows the S-parameter characteristics of the transmitting (S_{11}, S_{21}) and receiving (S_{22}, S_{12}) sides of identical SPDT-T/R switch structures. Fig. 3(b) shows the simulated S-parameter data of the two sides of SPDT-T/R module. The basic behaviours of the SPDT-T/R module for the two operation sides show wideband RF properties in terms of low transmission losses and high isolation.

2.3. 90° Hybrid Coupler

The hybrid coupler can act as a phase shifter to generate signals 90 degrees out of phase at its outputs to operate with I/Q signal for direct conversions. The hybrid coupler can generate signals 90 degrees out of phase at its output ports [10], while the port located on the same side as the input port is isolated. The proposed hybrid coupler design structure and simulation results are shown in Fig. 4.

From Fig. 4, at the frequency band from 1 GHz to 5 GHz, it is clear that the reflection coefficient, S_{11}, has a value -26.2 dB, and the transmission coefficients (S_{21}, S_{31}) have approximately $(-3.4, -3)$ dB which means that the power has been split relatively equal and that the isolation coefficient, S_{41}, has a value -24.4 dB, while at the frequency band from 5 GHz to 10 GHz, the behaviour has been changed with the frequency due to the relative change in the impedance matching.

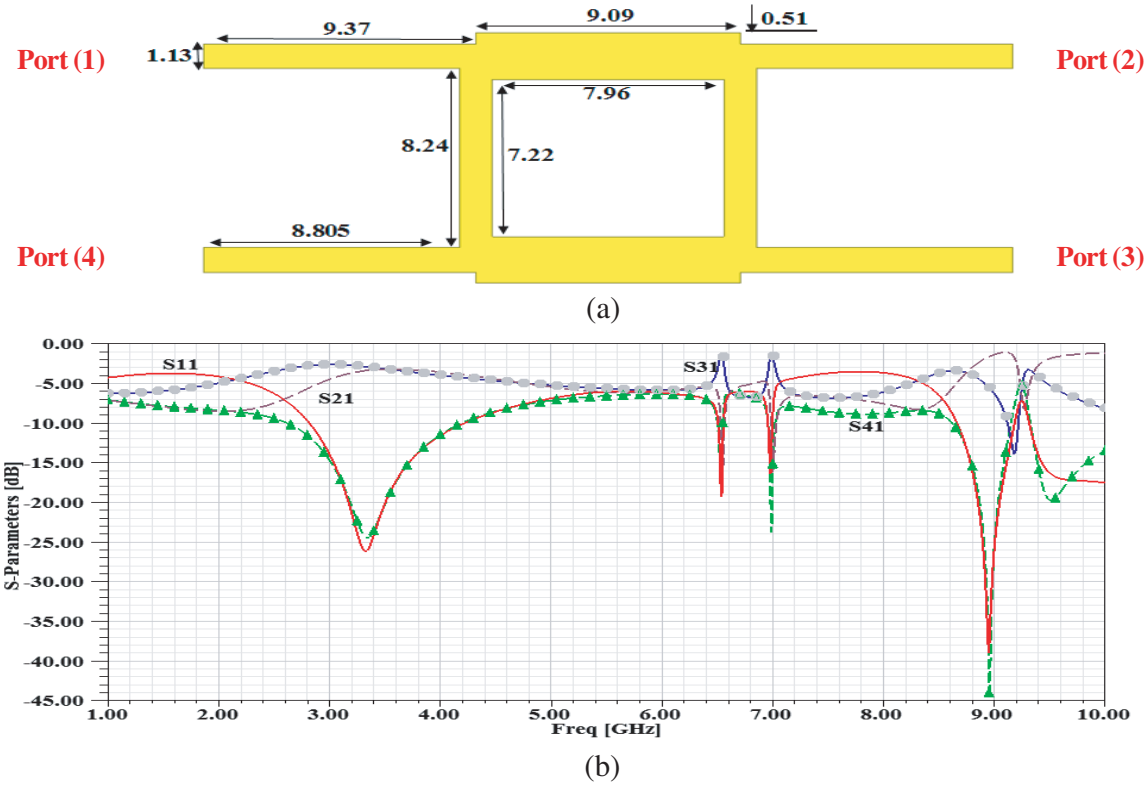

Figure 4. Proposed hybrid coupler and simulation results (all dimensions in mm). (a) Top view design structure. (b) S-parameters in dB.

2.4. Wilkinson Power Divider

The Wilkinson power divider is a device for splitting or combining signals [2]. It is composed of microstrip transmission lines and can be made with arbitrary power division with equally split 3 dB each port using quarter wavelength transmission line sections, as shown in Fig. 5.

From Fig. 5, at the frequency band from 1 GHz to 5 GHz, it is clear that the reflection coefficient, S_{11}, has a value -18.8 dB, and the transmission coefficients (S_{21}, S_{31}) have approximately $(-3.2, -3.2)$ dB, which means that the power has been split equally, while in the frequency band from 5 GHz to 10 GHz, the behaviour has been changed due to the relative change in the impedance matching. In the next section, the impedance matching will be maintained by adding a tuning stub to adapt the higher frequency band from 5 GHz to 10 GHz with the entire components of the proposed system.

2.5. Proposed MIMO-DCT System Structure

In wireless communications, MIMO has become an important technology due to diversity gain from the use of independent fading paths using multiple antennas. So, the signals received from multiple antennas must be combined coherently to improve the reception compared to the use of a single antenna [4].

The proposed integrated miniaturized MIMO-DCT system structure has been investigated, designed and simulated, as shown in Fig. 6.

Figures 6(a) and (b) show the proposed design structure and the signal flow graph, respectively. The S-parameters result of the proposed design structure is shown in Fig. 6(c) for the properly selected frequency band 2.7 GHz to 5.7 GHz. A sample of the far-field 3D polar plot, radiation patterns and gain for the proposed MIMO-DCT structure are also plotted, as shown in Fig. 6(d), which gives an intuitive insight into how the proposed structure operates.

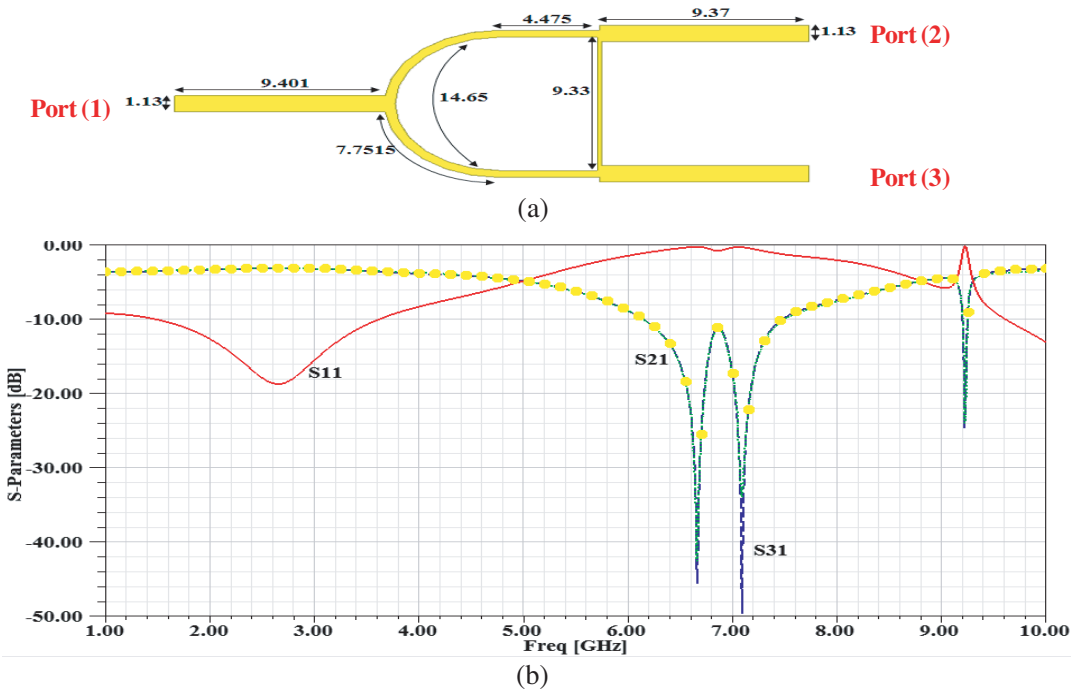

Figure 5. Proposed power divider and simulation results (all dimensions in mm). (a) Top view design structure. (b) S-parameters in dB.

3. PLANAR BUTLER MATRIX DESIGN STRUCTURE

The Butler matrix is normally employed in beam-forming and scanning networks for linear and conformal antenna arrays. So, the beam-forming will produce multi-beam of signal in each input port, each corresponding to a beam with its peak at a different angle in space. The Butler matrix network has N ports that are functionally divided into N inputs and N outputs, and can be described by an $N \times N$ scattering matrix [10–15]. Crossover coupler means crossing two transmission lines with minimal coupling between them. It can be observed that the planar implementation is made here as a cascade of two hybrid couplers. The proposed crossover coupler design structure and simulation results are shown

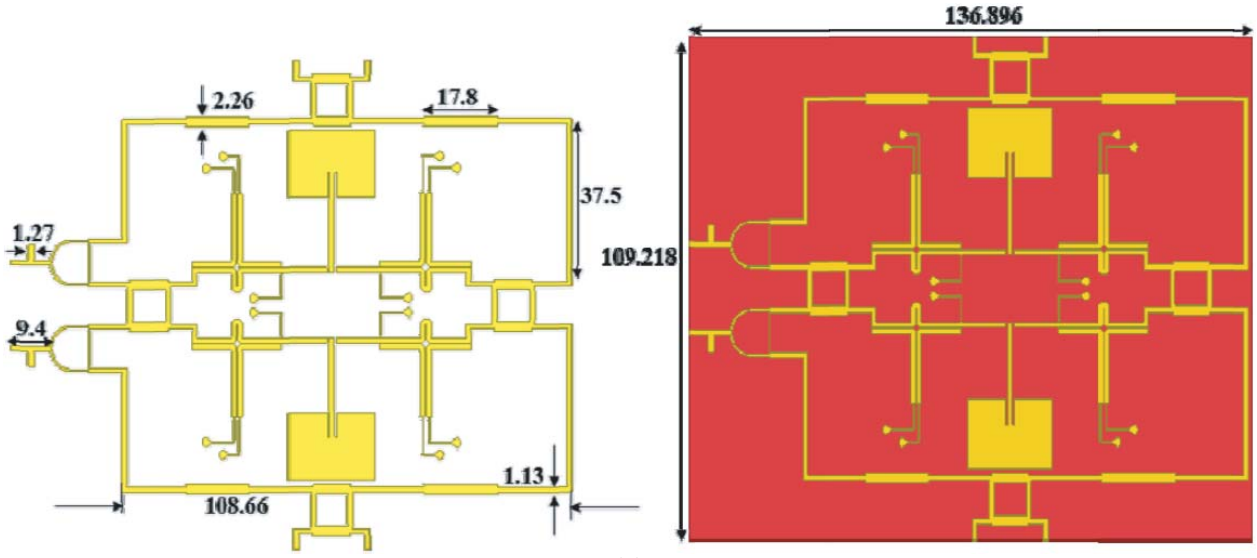

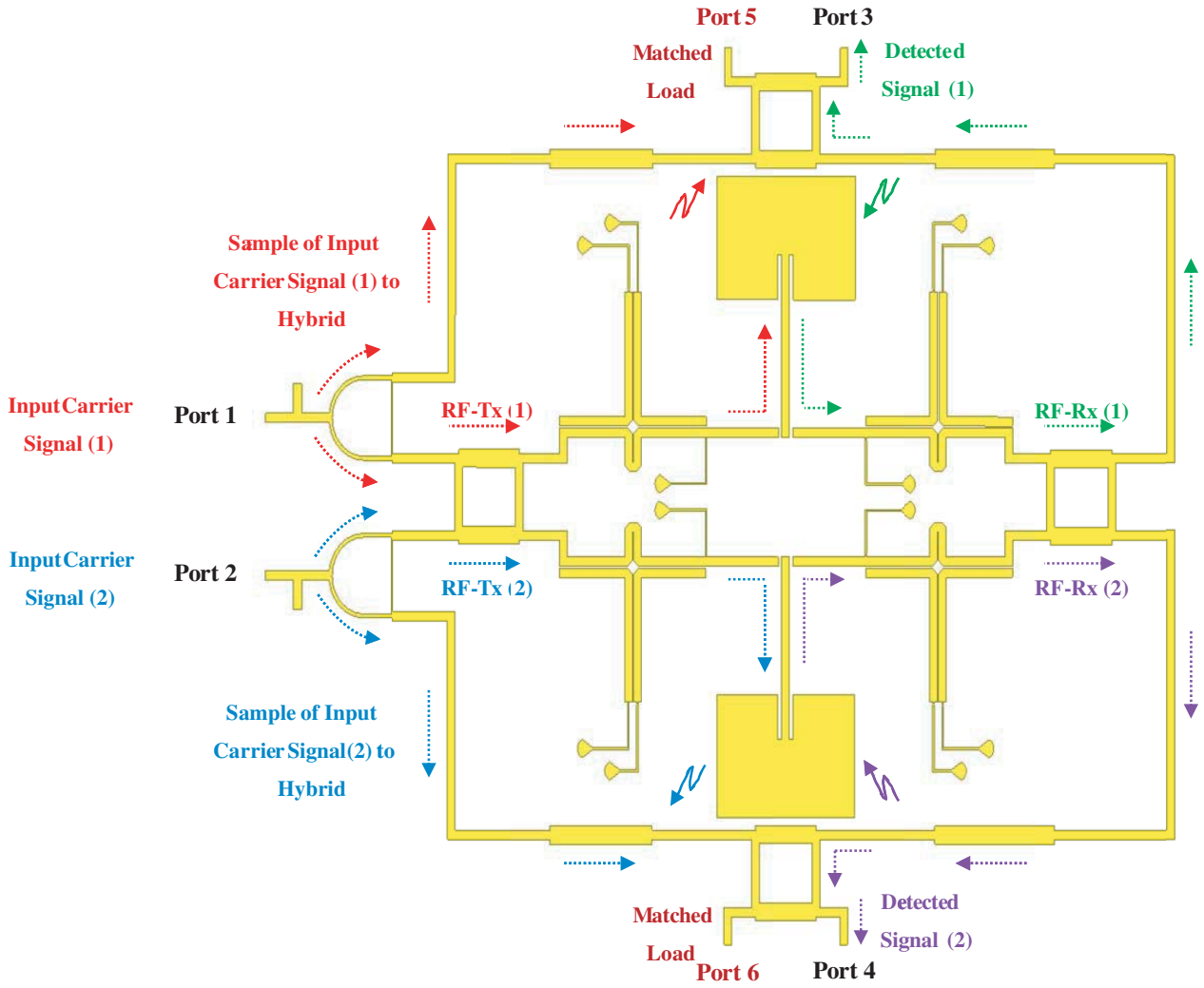
Port 5
Port 3
Matched
Load
Detected
Signal (1)
Sample of Input
Carrier Signal (1) to
Hybrid
Input Carrier
Signal (1)
Port 1
RF-Tx (1)
RF-Rx (1)
Input Carrier
Signal (2)
Port 2
RF-Tx (2)
RF-Rx (2)
Sample of Input
Carrier Signal (2) to
Hybrid
Matched
Load
Port 6
Port 4
Detected
Signal (2)

(b)

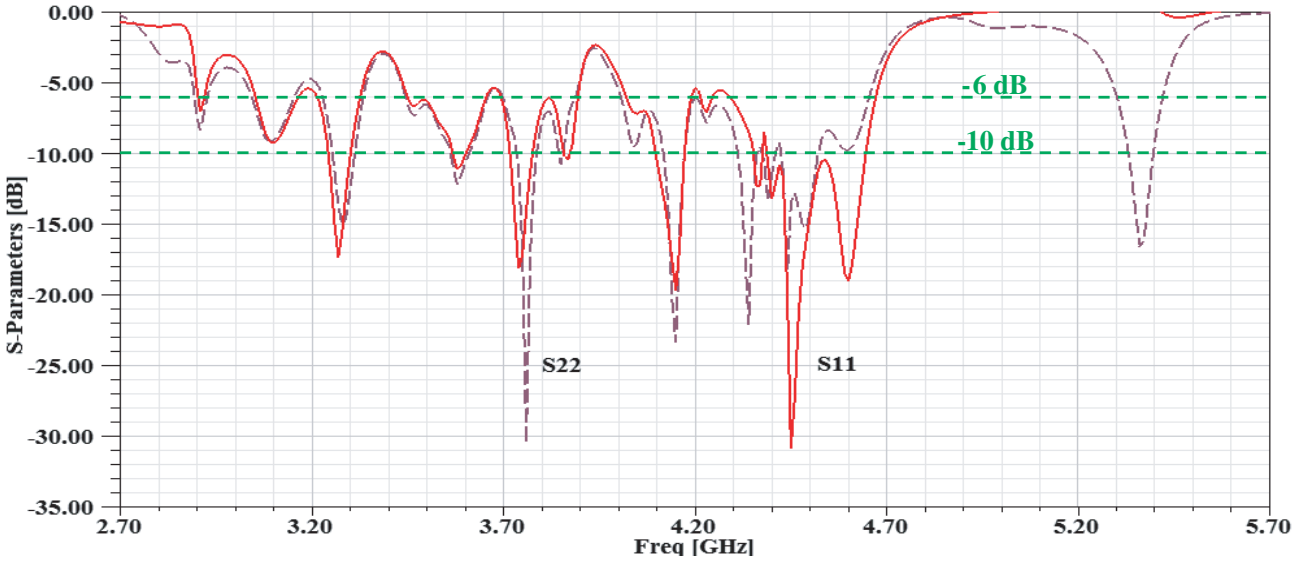
0.00
-5.00
-10.00
-15.00
-20.00
-25.00
-30.00
-35.00
S-Parameters [dB]
2.70
3.20
3.70
4.20
4.70
5.20
5.70
Freq [GHz]
-6 dB
-10 dB
S22
S11

(c)

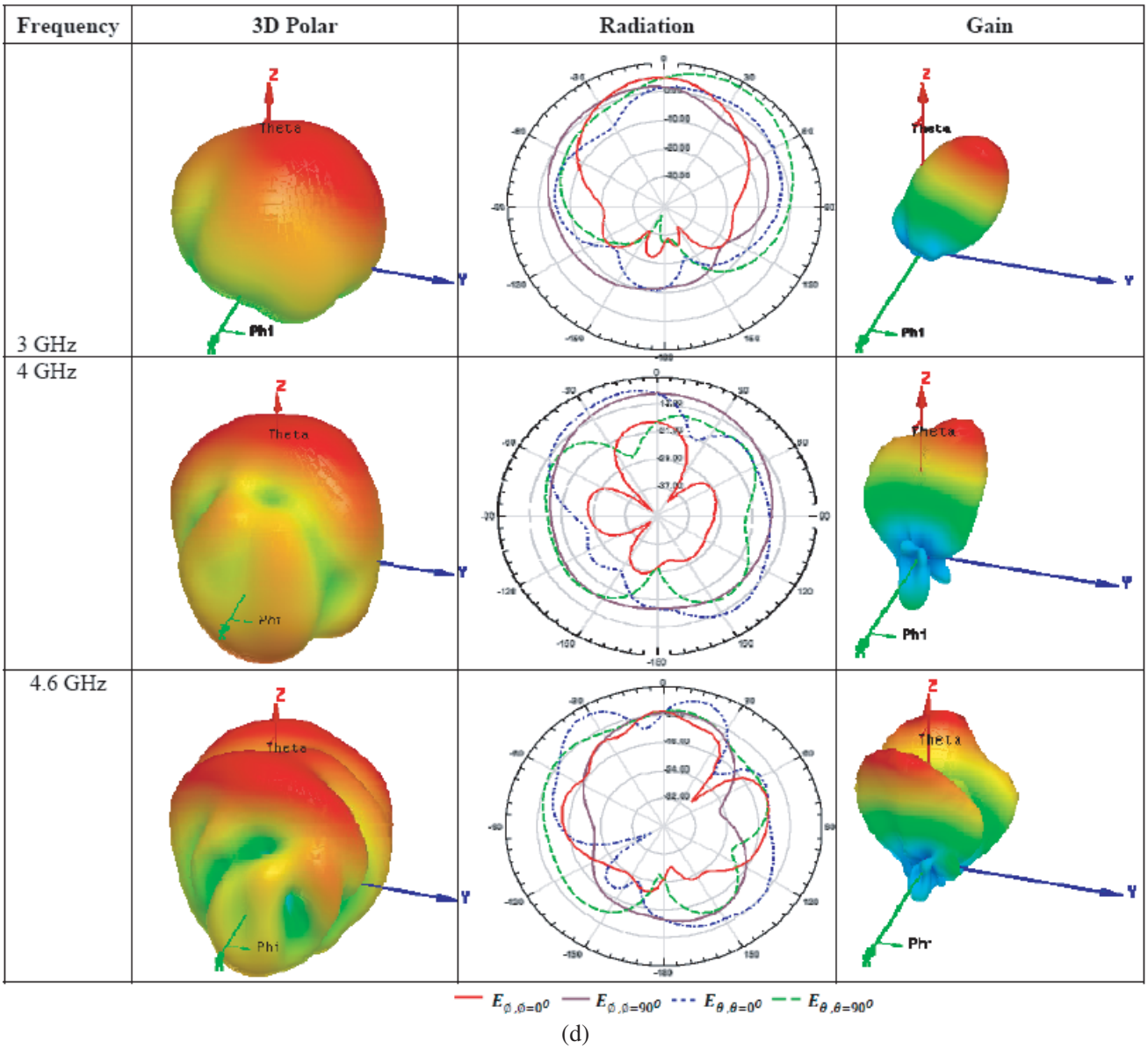

(d)

Figure 6. Proposed MIMO-DCT system structure and simulation results (all dimensions in mm). (a) 3D and top views. (b) The proposed MIMO-DCT system signal flow graph. (c) S-parameters in dB. (d) The Far field 3D polar, radiation patterns and gain for the proposed structure.

in Fig. 7.

The Butler matrix is designed, analysed, and the front view of the proposed structure and its optimum dimensions using parametric solution are shown in Fig. 8.

Numerical simulation is used to obtain the S-parameter characteristics of the proposed symmetrical planar Butler matrix design structure, as shown in Fig. 9.

From Fig. 9, it is clear that the proposed Butler matrix has a symmetrical design structure. So the simulated S_{11}, S_{22}, S_{33}, S_{44} in dB and the S-parameters in decibels of input ports on isolation demonstrate high isolation between the input ports versus frequencies in GHz. Also, due to the symmetrical design structure, samples of output ports (1) and (2) coupling are illustrated, respectively over the frequency band from 1 GHz to 10 GHz to give an intuitive insight into how the structure operates.

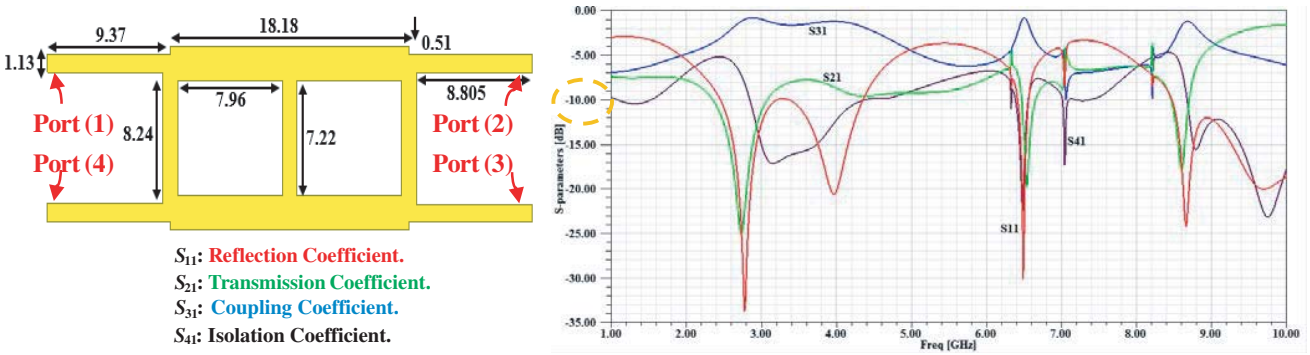

Figure 7. Proposed crossover coupler design structure (all dimensions in mm).

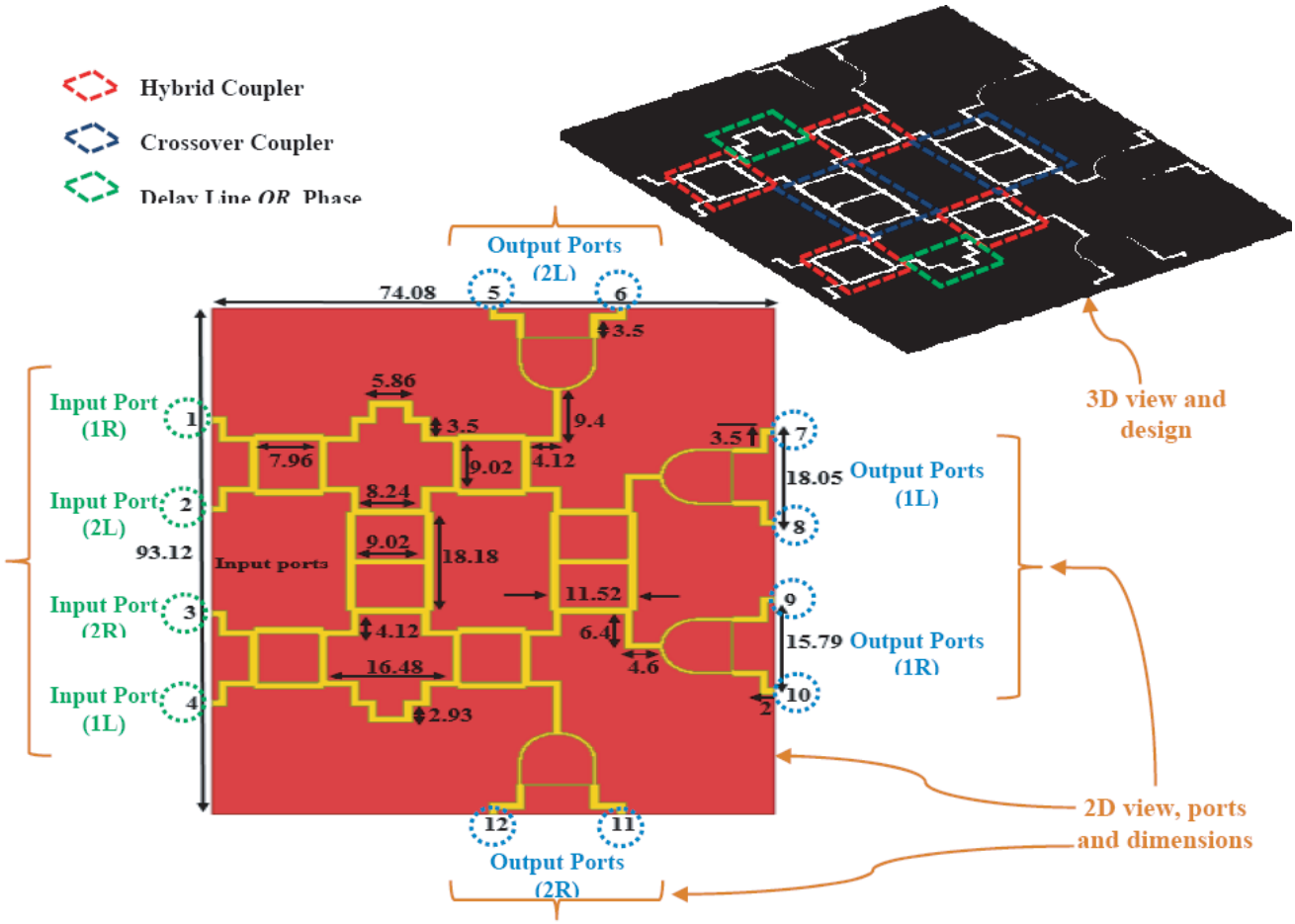

Figure 8. Proposed Butler matrix design structure (all dimensions in mm).

4. PROPOSED FULLY INTEGRATED MIMO-DCT WITH BUTLER MATRIX SYSTEM

The use of multiple antennas for both transmission and reception is associated with performance gains of fundamental nature. One such gain stems from the spatial-multiplexing capabilities of wireless MIMO channels [4]. The switched beam systems are traditionally designed to retrofit widely deployed Subarray MIMO-DCT systems. It has been commonly implemented as an add-on or application technology that intelligently addresses the needs of mature networks. The top view of the proposed fully integrated

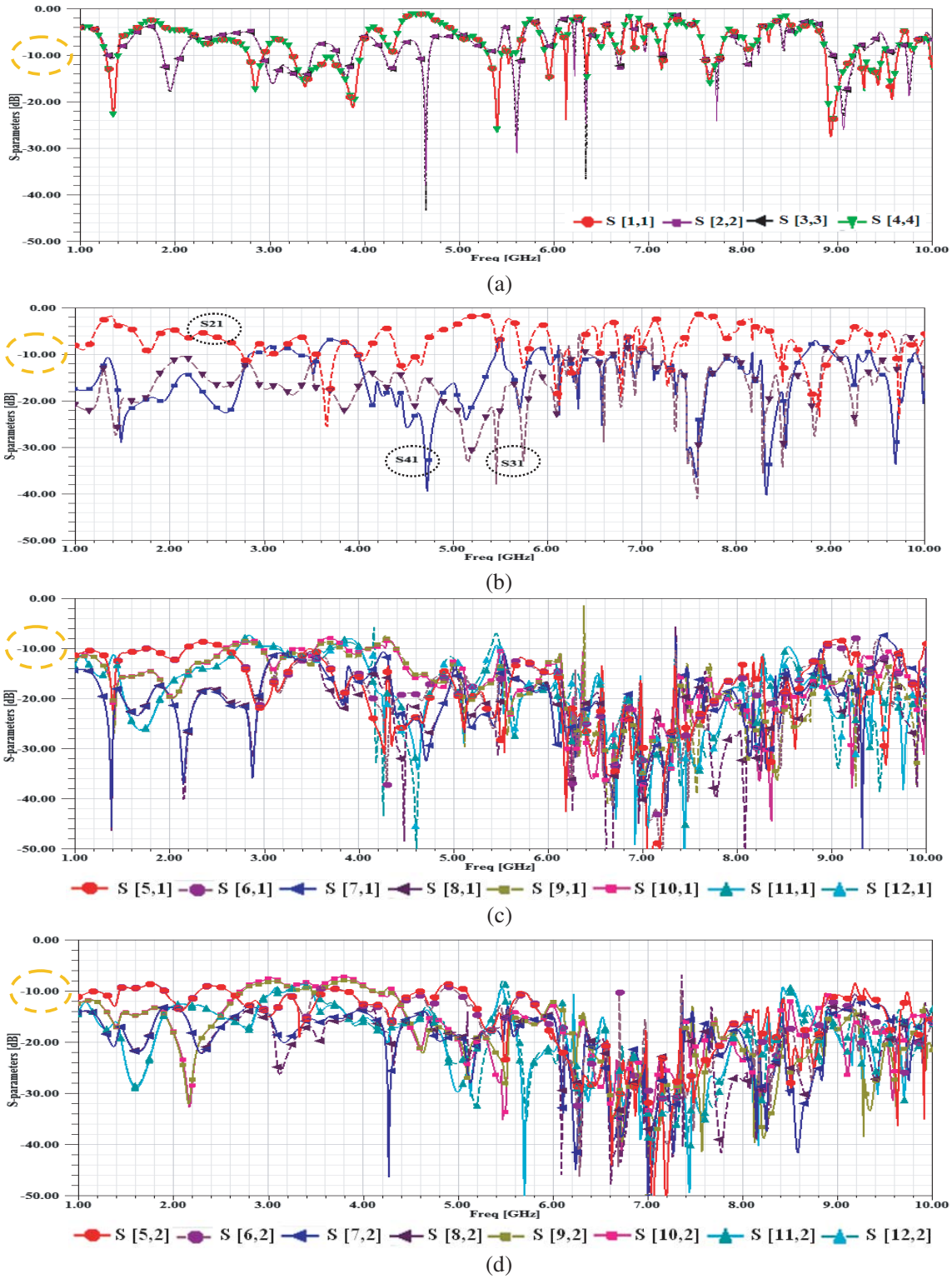

Figure 9. Simulated S-parameter characteristics of the proposed symmetrical planar Butler matrix. (a) Simulated S_{11}, S_{22}, S_{33} and S_{44} [dB] for input ports. (b) Simulated S-parameters on isolation [dB] for input ports. (c) Simulated S-parameters on coupling [dB] between input port (1) and output ports. (d) Simulated S-parameters on coupling [dB] between input port (2) and output ports.

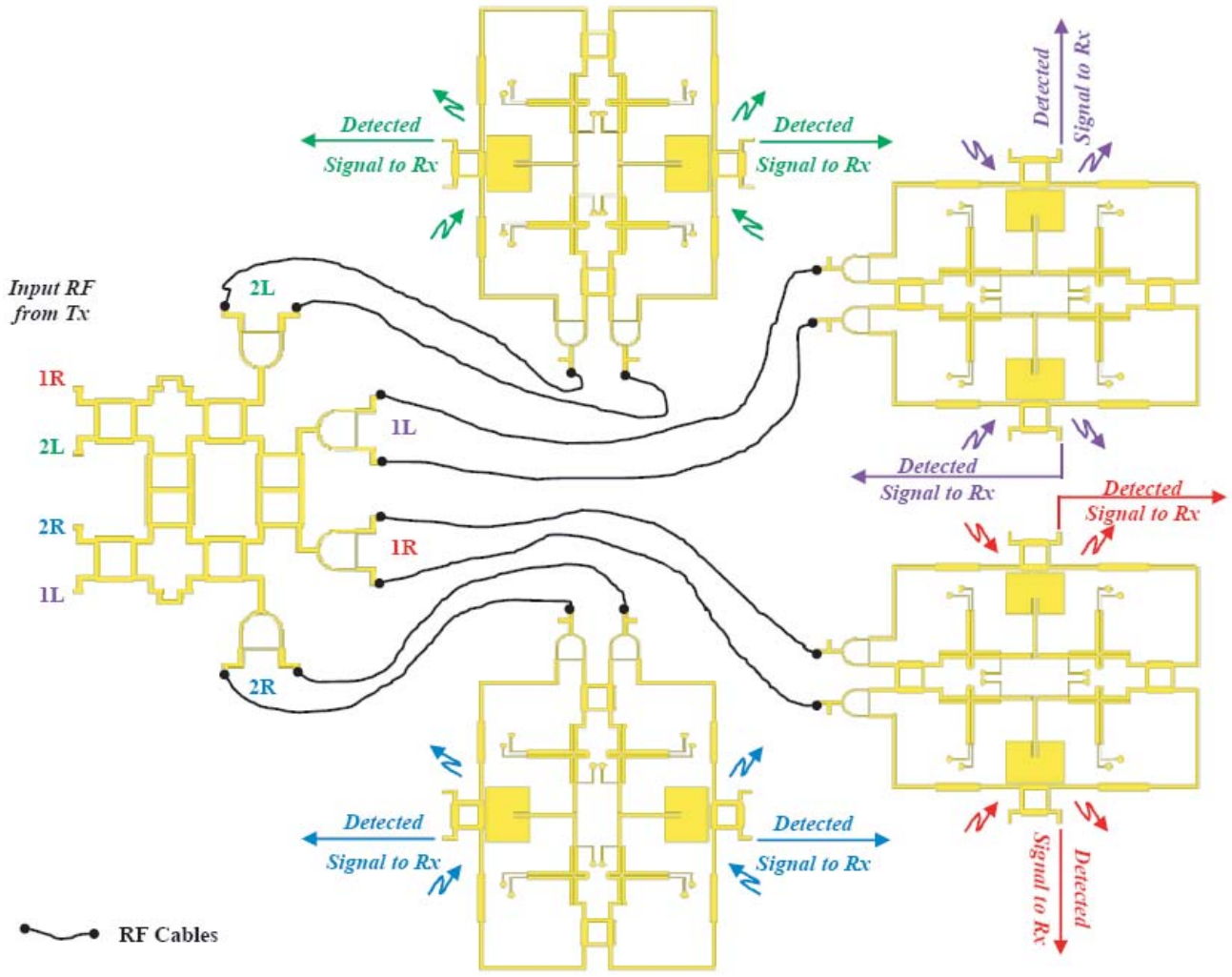

Figure 10. Proposed fully integrated MIMO-DCT with Butler matrix system structure.

system design structure is shown in Fig. 10.

Photographs of the proposed fabricated MIMO-DCT and the fully integrated system design structures at antenna laboratory and a sample of the measured S-parameters in dB of the proposed structures are analysed using an Agilent FieldFox network analyser, N9918A, as shown in Fig. 11.

From Figs. 9 and 11, it is clear that the measurement and simulation results are in a good agreement. The measured S_{11}, S_{22}, S_{33}, S_{44} in dB have different return loss values up to -55 dB related to the frequency in GHz. Also, the measured S-parameters in decibels of input ports on isolation demonstrate high isolation up to -50 dB between the input ports versus frequencies in GHz. The power patterns for each proposed MIMO-DCT demonstrate the relative radiation patterns in dB for the two output ports related to the input ports of the signals (1) and (2), respectively. Finally, the proposed fully integrated MIMO-DCT with a Butler matrix system design structure, shown in Fig. 10, was investigated and satisfied the main goal of miniaturized beam-switching array antenna over a frequency band from 1–10 GHz.

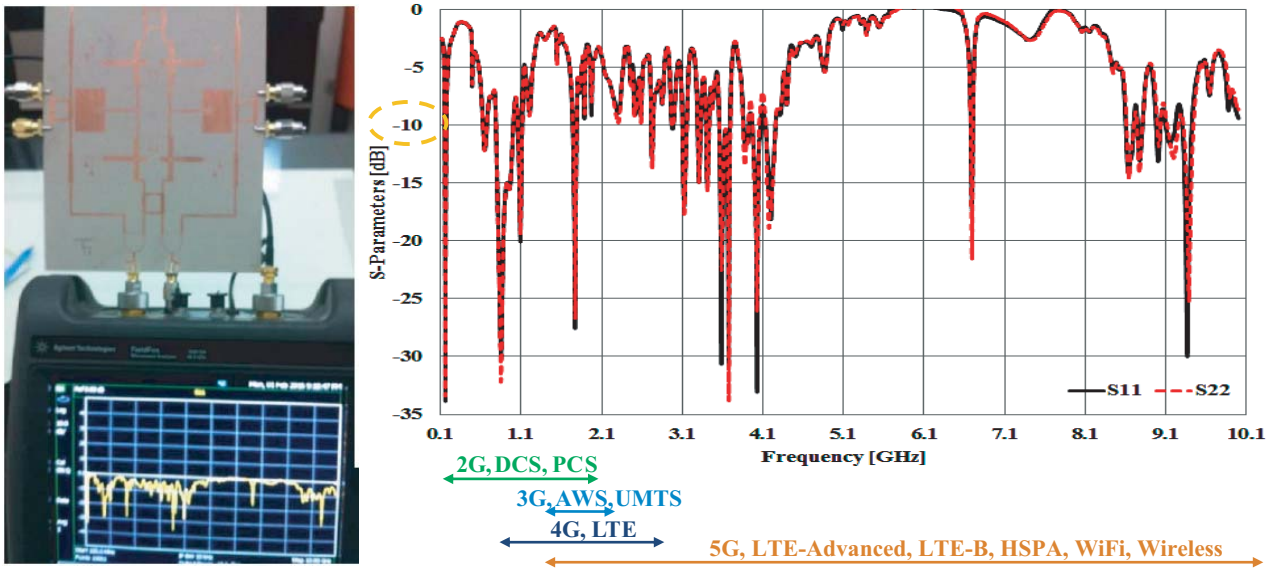
S-Parameters [dB]
0
-5
-10
-15
-20
-25
-30
-35
0.1
1.1
2.1
3.1
4.1
5.1
6.1
7.1
8.1
9.1
10.1
Frequency [GHz]
S11
S22
2G, DCS, PCS
3G, AWS, UMTS
4G, LTE
5G, LTE-Advanced, LTE-B, HSPA, WiFi, Wireless

(a)

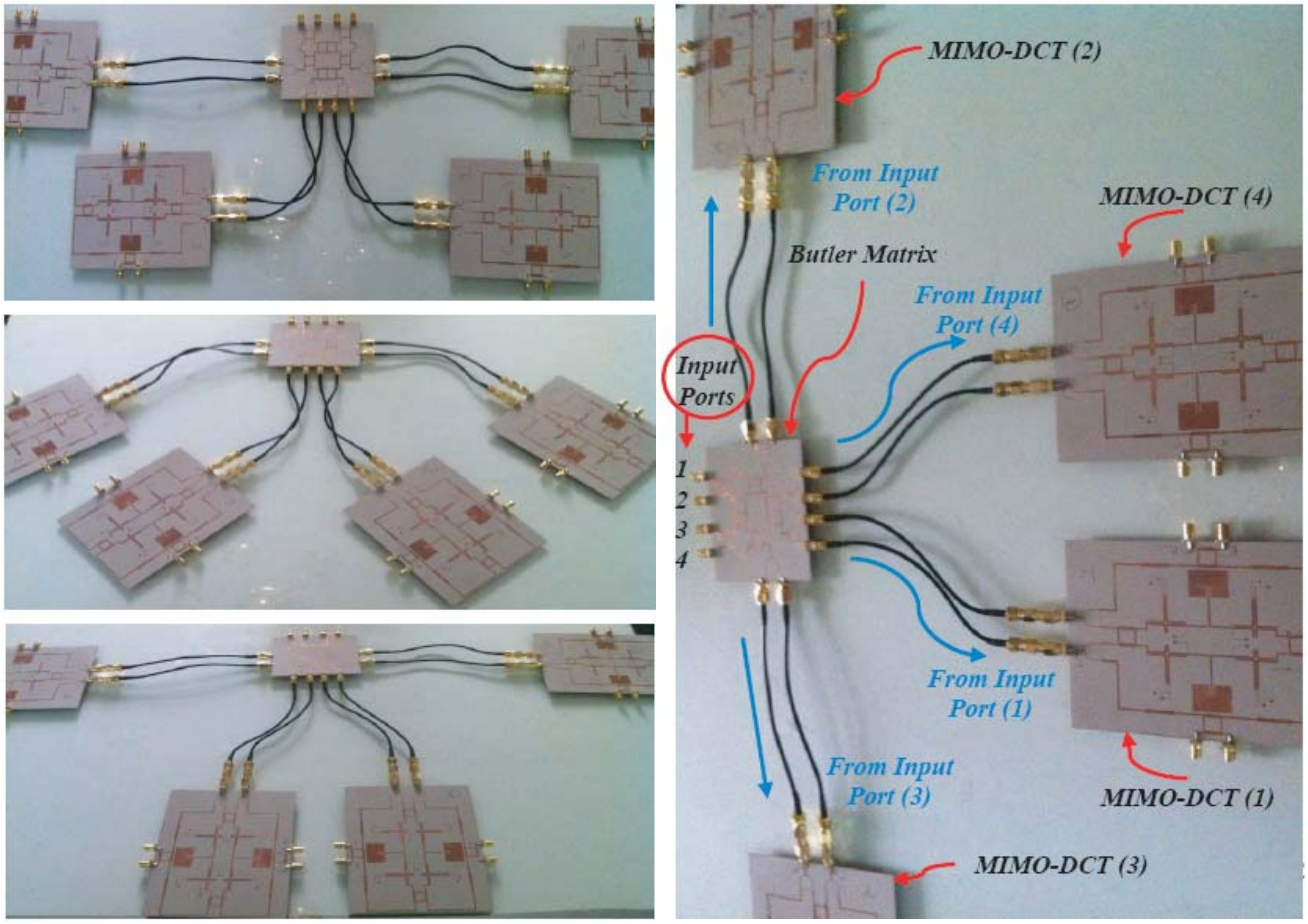
MIMO-DCT (2)
From Input Port (2)
MIMO-DCT (4)
Butler Matrix
From Input Port (4)
Input Ports
1
2
3
4
From Input Port (1)
From Input Port (3)
MIMO-DCT (1)
MIMO-DCT (3)

(b)

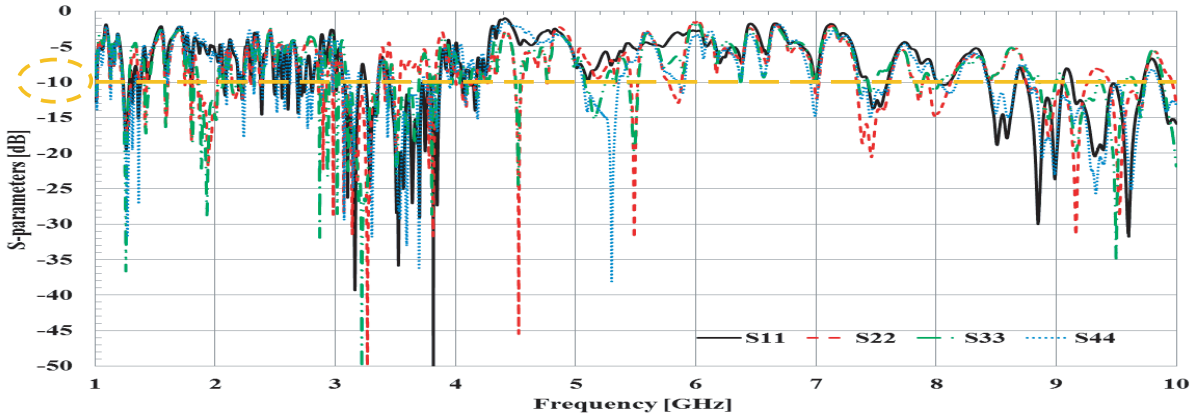

(c)

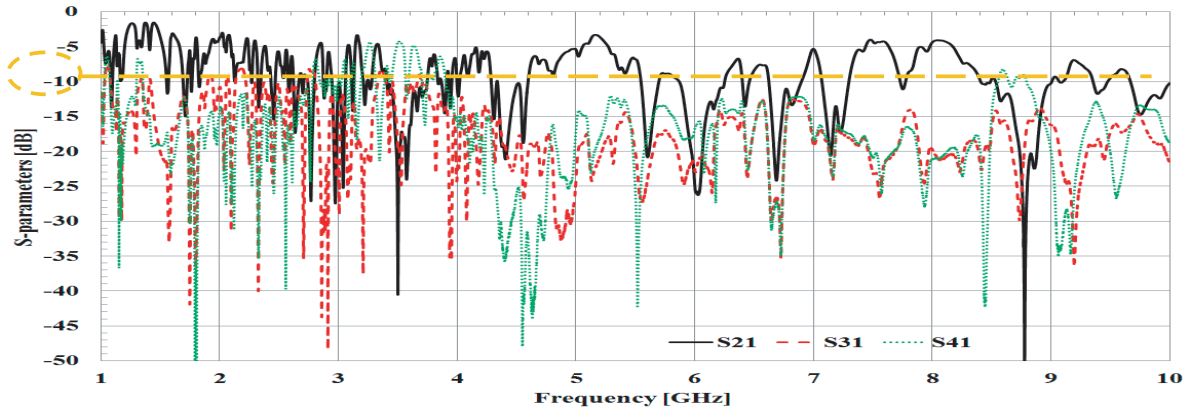

(d)

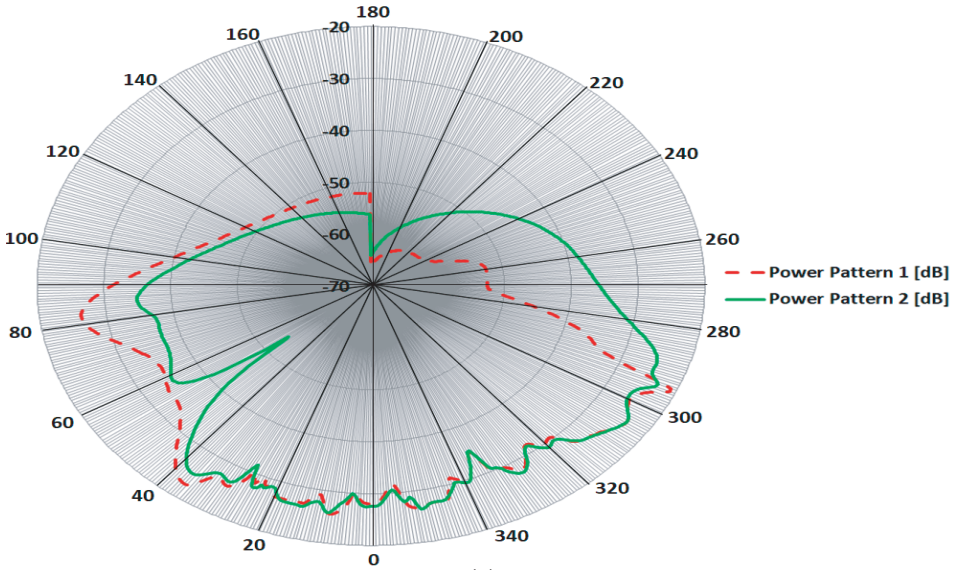

(e)

Figure 11. Fabricated and measured S-parameter characteristics of the proposed fully integrated system. (a) Fabricated MIMO-DCT structure and measurement results. (b) Fabricated fully integrated MIMO-DCT with Butler matrix system structure. (c) Measured S_{11}, S_{22}, S_{33} and S_{44} [dB] for input ports. (d) Measured S-parameters on isolation [dB] for input ports. (e) Measured power patterns [dB] for each proposed MIMO-DCT.

5. CONCLUSIONS

MIMO Direct conversion transceiver is a very promising architecture for high integration, low-cost, low-power and high performance. In an effort to develop single chip transceivers in order to reduce power dissipation and chip size, this paper investigates the design, fabrication, and analysis of a proposed miniaturized MIMO-DCT and the fully integrated system design structures. The simulated and measured characteristics have shown good agreement with the expected performance, compared with the traditional array design. The use of subarrays allows the array factor to be separated based on the geometry and excitation of subarrays. So, there are no losses other than those due to amplitude tapering. Then, the directivity and gain are approximately equal. The advantage of using a smart antenna system is better range or coverage which focuses the energy sent out and increases range and coverage. This is because the inputs from multiple antennas are combined to optimize available power required to establish given level of coverage. Moreover, switched beam antennas suppress interference arriving from directions away from the active beam's centre. They are normally used only for reception because of the system's ambiguous perception of the location of the received signal. It will make the consequences of transmitting in the wrong beam being obvious. The required angular accuracy and range resolution have been achieved with little limitation on platform space. Little perturbations in subarray locations do not have much effect on the array pattern. The arrangement and dimensions of the subarrays have been adjusted to achieve better performance. The proposed fully integrated MIMO-DCT with Butler matrix system provides high-resolution with high-speed data collection simultaneously and shows the tradeoff in performance and cost for several possible antenna concepts to meet the requirements for LTE and wireless communication applications.

REFERENCES

1. McTasney, R., D. Grunwald, and D. Sicker, "Low-latency multichannel wireless mesh networks," *Proceedings of the 16th Inter. Conf. on Computer Comm. and Networks (ICCCN'2007)*, 1082–1087, 2007.
2. Madany, Y. M. and A. A. Salama, "Design and analysis of miniaturized integrated antenna with direct conversion transceiver for wireless communications applications," *Inter. Conf. on Microwave and Millimeter Wave Technology (ICMMT'2012)*, 1–4, May 2012.
3. Madany, Y. M., N. E. H. Ismail, and H. A. Hassan, "High-isolation wideband single-pole double-throw (SPDT) transmitter/receiver (T/R) switch with PIN diode for wireless communication applications," *IEEE Inter. Symp. on Ant. and Propag. (APS'2013)*, 1006–1007, July 2013.
4. Palomar, D. P., J. Cioffi, and M. Lagunas, "Joint Tx-Rx beam forming design for multicarrier MIMO channels, A unified framework for convex optimization," *IEEE Trans. Signal Process.*, Vol. 51, No. 9, 2381–2401, 2003.
5. Yin, H., D. Gesbert, M. Filippou, and Y. Liu, "A coordinated approach to channel estimation in large-scale multiple-antenna systems," *IEEE Journal on Selected Areas in Communications*, Vol. 31, 264–273, 2013.
6. Sharawi, M. S., S. K. Podilchak, and K. Sarabandi, "Compact millimeter-wave switched-beam antenna arrays for short range communications," *Microwave and Optical Technology Letters*, Vol. 58, No. 8, 1917–1921, August 2016.
7. Tiwari, N. and T. R. Rao, "A switched beam antenna array with Butler matrix network using substrate integrated waveguide technology for 60 GHz radio," *ACES Journal*, Vol. 31, No. 5, 599–602, May 2016.
8. Tiwari, N. and T. R. Rao, "A switched beam antenna array with Butler matrix network using substrate integrated waveguide technology for 60 GHz wireless communications," *International Journal of Electronics and Communications, (AEU)*, Vol. 70, 850–856, 2016.
9. Erfani, E., E. Moldovan, and S. Tatu, "A 60-GHz multi-beam antenna array design by using MHMICs technology," *Microwave and Optical Technology Letters*, Vol. 58, No. 8, 1844–1847, August 2016.

10. Shastrakar, A. and U. S. Sutar, "Design and simulation of microstrip Butler matrix elements operating at 2.4 GHz for wireless applications," *International Journal of Scientific & Engineering Research*, Vol. 7, No. 5, 1528–1531, May 2016.
11. Suryana, J., A. Y. Pinangkis, and A. Nursyamsiah, "Design and implementation of 3-D multi-beam antenna and FMCW S-band radar for fire control system," *Asian Research Publishing Network (ARPN) Journal of Engineering and Applied Sciences*, Vol. 11, No. 5, 3176–3183, March 2016.
12. Hirokawa, J. and D.-H. Kim, "Waveguide short-slot 2D-plane coupler for 2D beam-switching Butler matrix," *The 3rd AWAP 2016*, 30, January 27–29, 2016.
13. Kalam, S. V. and A. B. Rathi, "Optimum design of 4×4 symmetrically structured Butler matrix," *International Journal of Scientific Research Engineering & Technology (IJSRET)*, Vol. 5, No. 1, 31–34, January 2016.
14. Karamzadeh, S. and M. Kartal, "Circularly polarized 1×4 square slot array antenna by utilizing compacted modified Butler matrix and branch line coupler," *International Journal of RF and Microwave Computer-Aided Engineering*, Vol. 26, No. 2, 146–153, Wiley Periodicals, Inc., February 2016.
15. Madany, Y. M., H. M. Elkamchouchi, and A. A. Salama, "Investigation and design of distributed subarray smart antenna system using 1×8 switched Butler matrix for phased-array radar applications," *Inter. Conf. on High Speed Intelligent Communication (HSIC'2012)*, 279–282, May 2012.